Modelling and Analysis of Off-Road Rally Vehicle using Adams Car

Shreyas B N[1], Kiran M D[2]

[1, 2]*Department of Mechanical Engineering, B.M.S Institute of Technology and Management, Yelahanka, Bangalore, India*

***Abstract*—The paper discusses the modelling of a virtual prototype of the suspension and steering sub systems of a physical rally vehicle available on campus. Upon modelling the front and rear suspensions and the steering on Adams Car, the created model is tested for its correctness using Half Vehicle analysis like K and C analysis, and full car analysis like CRC and Maintain Analysis. Furthermore, the front lower control arm is made flexible to see the stresses acting on it to investigate its reason for failure in the actual prototype.**

***Keywords*-Kinematics; camber; toe; caster; cornering; maintain; flex body**

I. INTRODUCTION

An off-road vehicle, as the name suggests, is usually driven on uneven terrains and harsh road conditions.For this project, the rally car has been built with handling properties being given the utmost priority. The chassis is fabricated with steel as the material. The front suspension used it of the double wishbone type, falling under independent type of suspensions. The rear suspension resembles the multilink type. There are 6 suspension struts used in this car. Two are used in front suspension and four struts are used at the rear suspension. The main aim in this project is to find out the reason of failure of the control links in the front suspension.

Figure 1.1 Physical prototype of rally car

II. MODELLING THE VIRTUAL PROTOTYPE USING ADAMS CAR

The aim of this project is to dynamically analyze the performance of the off-road vehicle by creating a replica of the physical suspension model on the software GUI. This phase is crucial as small errors in the data procured can lead to large changes in the dynamic behavior of the car. Hence, utmost care has to be taken to ensure the hard points extracted from the physical prototype are as accurate as possible.

Once the hard points are fed into ADAMS Car Template Builder, the modelling is progressed by defining parts for the created hard points, creating geometry for the defined parts, assigning relative motion between the created parts by creating joints and bushings where ever required. The mass and inertia properties of individual parts are unavailable on the physical prototype due to various domestic constraints.

The following steps are followed in order to model the suspension accurately.

- Hard Points
- Defining Parts
- Creating Geometry
- Creating Joints and Bushes
- Assigning Communicators

III. MODELLING THE SUSPENSION SUBSYSTEMS

A. Creating the Front Suspension.

The following table shows the different hard points that have been extracted for front suspension template. All the measurements are made in Cartesian co-ordinates.

		FS	
		HP	
Part	**X**	**Y**	**Z**
Drive Shaft Inner	0	-200	225
Lca Front	-140	-320	170
Lca Outer	45	-800	220
Lca Rear	95	-345	180
Lower Strut Mount	-40	-625	325
Subframe Front	-140	-320	170
Subframe Rear	95	-345	180
Tierod Inner	200	-400	300
Tierod Outer	120	-730	360
Top Mount	220	-450	860
Uca Front	-140	-350	315

Uca Outer	-60	-675	330
Uca Rear	85	-365	320
Wheel Center	0	-840	310

Table 3.1 Hard points of front suspension all in mm.

Upon completion of the entire process, the template of front suspension is completed and shown in figure. The car uses double wishbone suspension in the front with rack and pinion steering arrangement.

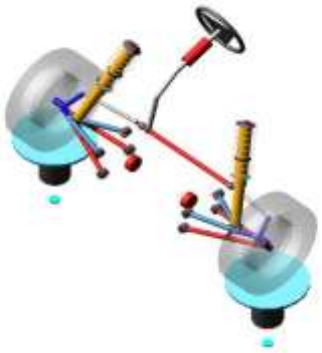

Figure3.1 Isometric View of Front Suspension

B. Creating Rear Suspension.

The rear suspension modelling is done in the same way as the front suspension. The rear suspension largely resembles the multi-link suspension system. There are a few modifications made to the multi-link suspension to closely represent the suspension used in the rally car as much as possible. They are,

- An extra suspension strut is added at the exact location used in the physical prototype.
- The lateral bar is removed as this part isn't present in the actual car.
- Control arm is also removed in the virtual prototype to closely resemble the physical car.
- The location of every part is accurately assigned.

The following image shows the rear suspension.

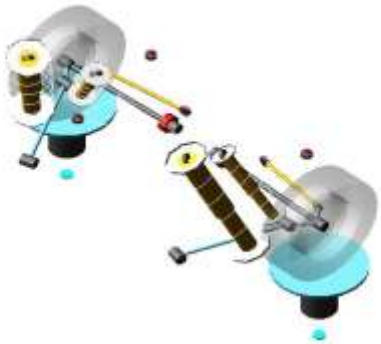

Fig 3.2 Isometric View of Rear Suspension

C. Creating Assembly

The front suspension which resembles the double wishbone is modelled completely. The steering of rack and pinion type is also modelled.

The rear suspension resembling multi-link suspension is modelled and several changes are made to the model too. Once everything is complete, all the sub systems are called into an assembly including the powertrain and chassis.

The powertrain, chassis and tires are used from the Adams Car library. The full assembly of the car is as shown in figure.

Figure 3.3 Full Vehicle Assembly

IV. KINEMATICS AND COMPLIANCE ANALYSIS

The virtual models of suspension system have to be proven that they are correctly modeled. Correlations can be made by comparing the simulated results with the experimental results. In this project, the model will be built on ADAMS Car and the simulated results are generated. The experimental results are tough to procure due to financial constraints, although these results can be used for verification if the car is analyzed for K and C experimentally in the future.

Figure 4.1 K and C test rig for physical prototypes.

The purpose of performing K and C is to develop and simulate a fully working MBD suspension model of the actual Off-Road Rally Car present in the campus, of Double Wishbone type as the front suspension and the multilink type

for the rear suspension systems. Both the simulated and experimental results only consider the value of the toe change, camber change and wheel rate when subjected to the Vertical In-Phase Test and Vertical Anti-Phase test.

D. Front Suspension K and C Analysis.

Suspension kinematics analysis is the most important part of the chassis tuning, and it is the basic guarantee to ensure the vehicle to control stability. The process is widely referred to as K and C (Kinematics and Compliance) analysis or half vehicle analysis. Joints are used during kinematic analysis and bushes are used during compliance analysis. The MBD models of the double wishbone front suspension and rack and pinion steering systems are established in ADAMS Car, and the model is used to analyze the following:

- Wheel rate
- Toe change
- Camber change

The front suspension along with the wheel and steering is set up on a two post-test rig on ADAMS Car. The different uneven road maneuvers are replicated on the software and plots are made to observe the above mentioned characteristics of the suspension. The different analyses used are as follows:

- Vertical In-Phase
- Vertical Anti-Phase

The following calculations show how preload has been decided.

Total Mass = 312 Kg

Unsprung Mass = 72 Kg

Therefore, Sprung Mass = 240 Kg

Weight distribution = 49:51

Therefore, Front axle load = 0.49*240

Wf = 117.6 Kg acting on two springs.

Therefore, preload on each spring = 117.6/2 = 58.8 Kg

Preload = 58.8*9.81 = 576 N

For the front suspension, we will carry out two simulations. The two being Vertical In-Phase and Vertical Anti-Phase tests. In Vertical In-Phase, the two posts of the test rig lift both wheels and drops them with zero phase lag between the wheels. In Vertical Anti-Phase, while the left wheel experiences bump travel, the right wheel will undergo rebound and vice versa.

The input is given as bounce and rebound. Once the simulation is complete, with the help of ADAMS Post Processor, the kinematics and dynamics of the suspension subsystem are analyzed. Any modifications made to the suspension parameters will be done to achieve better stability of the car.

Analysis Type	K and C
Vehicle	Off Road Rally Vehicle
Spring Stiffness	47 N/mm
Preload	576 N
Wheel Load	18 Kg
Bump	55 mm
Rebound	-30 mm

Table 4.1 K and C Input for Front Suspension

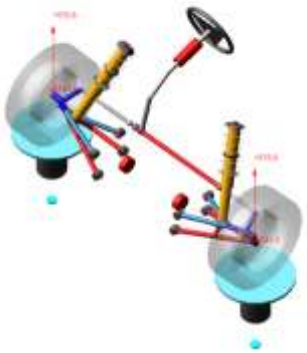

Figure 4.2 K and C Vertical In-Phase at Front Suspension.

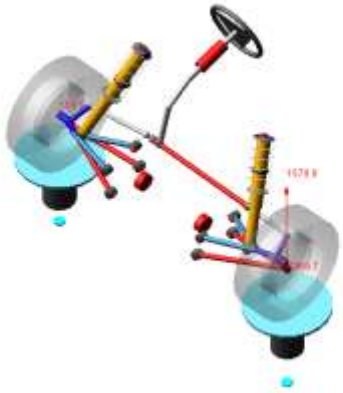

Figure 4.3 K and C Vertical Anti-Phase at Front Suspension.

Wheel Rate

Wheel rate is the vertical stiffness of the suspension relative to the body, measured at the wheel center.

Theoretical Calculation of Wheel Rate

Wheel Rate can be calculated using the relation,

Wheel Rate=Spring Rate * (Motion Ratio ^ 2) * Spring Angle Correction N/mm.

Spring Rate = 47 N/mm

Motion Ratio = Arm Distance/ Wheel Distance = 305/520 = 0.5865

Spring Angle Correction = cos (18 deg) = 0.9510

Therefore, Wheel Rate = 47*0.35*0.9510

Wheel Rate (Theoretical Value) = 15.7 N/mm

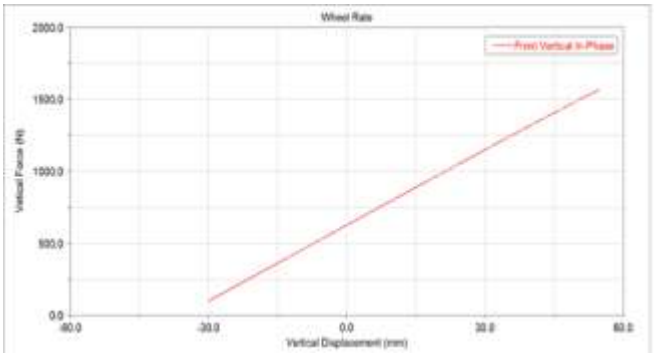

Figure 4.4 Wheel Rate for Front suspension during Vertical In-Phase.

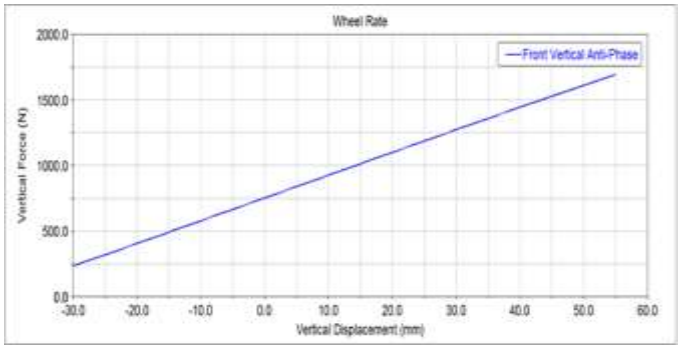

Figure 4.5 Wheel Rate for Front suspension during Vertical Anti-Phase.

Here, the vertical force applied at the left (or right) tire is observed to vary almost linearly to the vertical displacement of the left (or right) tire.

- From the graph, the wheel rate is observed to be equal to 16.39 N/mm.
- This value conforms closely with the calculated value i.e., 15.7 N/mm.
- The slope of the line gives the value of wheel rate in N/mm.
- At 55 mm displacement, i.e., during bump travel, the vertical force at left tire will increase to 1570.88 N.
- When the left wheel rebounds to the full extent i.e, -30 mm, the vertical force at left tire decreases to almost 99.2048 N.

Camber Change

Camber angle is the angle (in degrees), between the perpendicular from the ground and the center line of the wheel, as seen from car's front. If the center line is inclined inwards, it is called negative camber, and if it is inclined outwards, it is called positive camber.

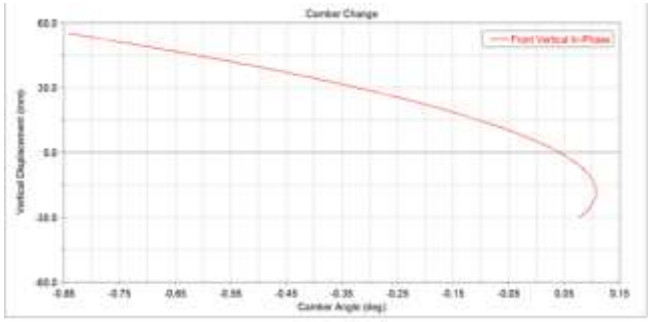

Figure 4.6 Camber Change for Front suspension during Vertical In-Phase.

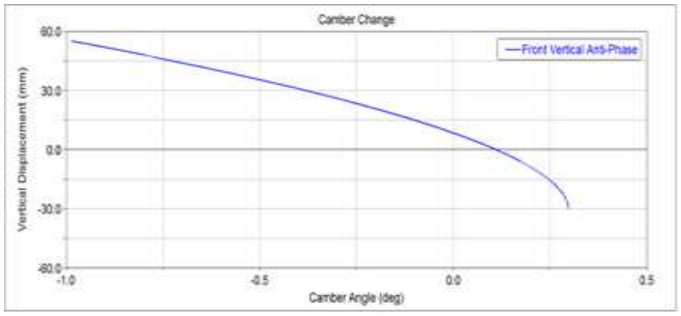

Figure 4.7 Camber Change in Front suspension during Vertical Anti-Phase.

Above graph shows a non-linear relationship between camber angle and vertical wheel travel when both wheels are displaced in-phase and anti-phase with the given values of bump and rebound.

- From the graph it is observed that the wheels will be in negative camber set up for most of its travel, which is desirable in most vehicles as they provide great cornering response.
- When the wheel bumps to an extent of 55 mm in vertical direction, the camber angle will decrease to -0.8417 degrees.
- When the wheel rebounds to an extent of -30 mm in vertical direction, the camber angle will increase to 0.0775 degrees.

Toe Change

The toe angle is the angle to which the wheels are out of parallel, or angle of wheel centerline along the length of the vehicle.

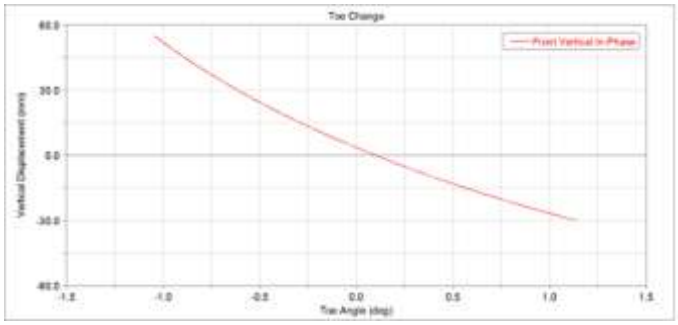

Figure 4.8 Toe Change for Front suspension during Vertical In-Phase.

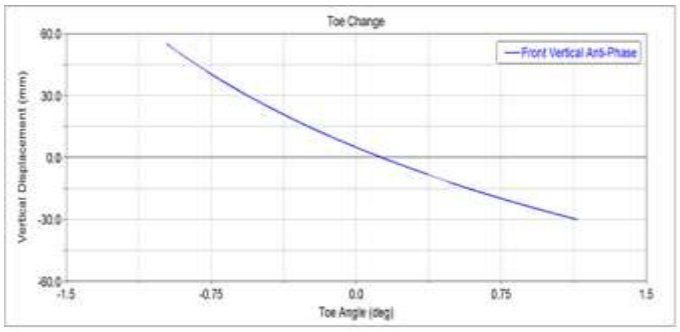

Figure 4.9 Toe Change for Front suspension during Vertical Anti-Phase.

The above graph shows a non-linear relationship between toe angle and vertical wheel travel when both wheels are displaced in-phase and anti-phase with the given values of bump and rebound. From the graph, it can be observed that:

- When the wheel bumps to an extent of 55 mm in vertical direction, the toe angle will increase to -1.0448 degrees.
- When the wheel rebounds to an extent of -30 mm in vertical direction, the camber angle will decrease non-linearly to 1.1391 degrees.
- Bump results in Toe-out which helps the vehicle to negotiate corners faster and offers less straight line stability.
- Rebound results in Toe-in which is preferred for passenger vehicles as they offer straight line stability. It also helps in achieving under steer characteristics.

E. Rear Suspension K and C Analysis

The MBD model of the multilink rear suspension is established in ADAMS Car, and the model is used to analyze the following:

- Wheel rate
- Toe change
- Camber change

The rear suspension along with the wheels is set up on a two post-test rig on ADAMS Car. The different uneven road maneuvers are replicated on the software and plots are made to observe the above mentioned characteristics of the suspension. The different analyses used are as follows:

- Vertical In-Phase
- Vertical Anti-Phase

The following calculations show how preload has been decided.

Total Mass = 312 Kg

Unsprung Mass = 72 Kg

Therefore, Sprung Mass = 240 Kg

Weight distribution = 49:51

Therefore, Rear Axle Load = 0.51*240

Wr = 122.4 Kg acting on four springs.

Therefore, preload on each spring = 122.4/4 = 30.6 Kg

Preload = 30.6*9.81 = 300.18 N

For the rear suspension as well, we will carry out two simulations. The two being Vertical In-Phase and Vertical Anti-Phase tests. In Vertical In-Phase, the two posts of the test rig lift both wheels and drops them with zero phase lag between the wheels. In Vertical Anti-Phase, while the left wheel experiences bump travel, the right wheel will undergo rebound and vice versa. The input is given as bounce and rebound.

Analysis Type	K and C
Vehicle	Off Road Rally Vehicle
Spring Stiffness	47 N/mm
Preload	300.18 N
Wheel Load	18 Kg
Bump	55 mm
Rebound	-15 mm

Table 4.2 K and C Input for Rear Suspension

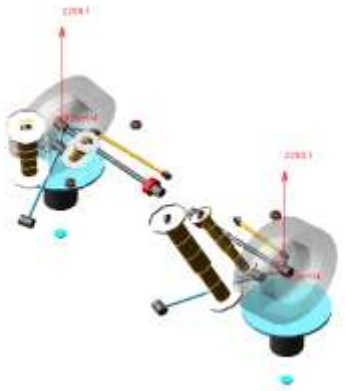

Figure 4.10 K and C Vertical In-Phase at Rear Suspension.

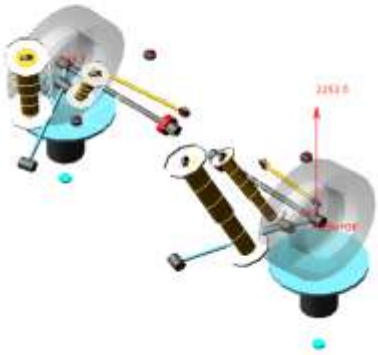

Figure 4.11 K and C Vertical Anti-Phase at Rear Suspension.

Wheel Rate

Wheel rate is the vertical stiffness of the suspension relative to the body, measured at the wheel center. The curve, for both cases, is observed as shown in the graphs.

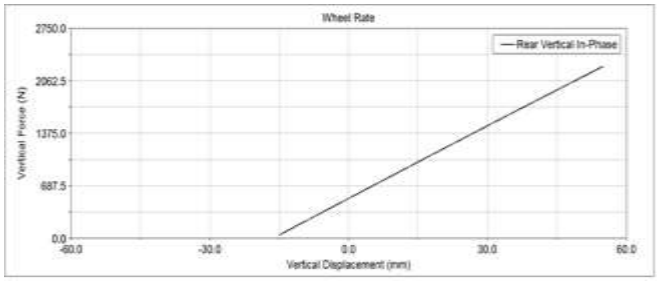

Figure 4.12 Wheel Rate for Rear suspension during Vertical In-Phase.

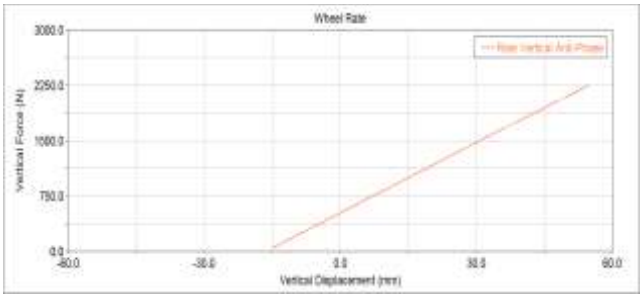

Figure 4.13 Wheel Rate for Rear suspension during Vertical Anti-Phase.

Here we observe that the vertical force applied at the left (or right) tire varies almost linearly as the vertical displacement of the left (or right) tire.From the graph, we can observe the following:

- The wheel rate from the plot is found to be 30.83 N/mm.
- At 55 mm displacement, i.e., during bump travel, the vertical force at left tire will increase to 2253.45 N.
- When the left wheel rebounds to the full extent i.e., -15 mm, the vertical force at left tire decreases to almost 39.18 N.

Camber Change

The change in the camber angle is significantly high in rear suspension as it is missing crucial elements like control arm and lateral link. It is clearly observed in the graphs below during both cases.

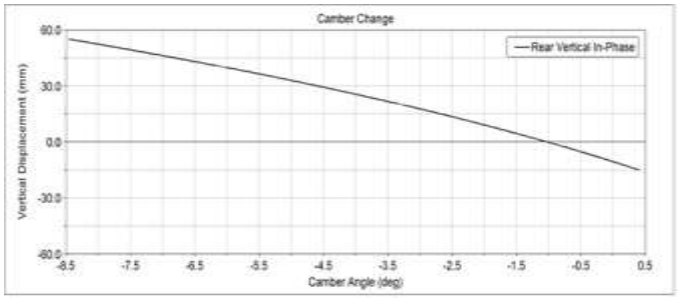

Figure 4.14 Camber Change for Rear Suspension during Vertical In-Phase.

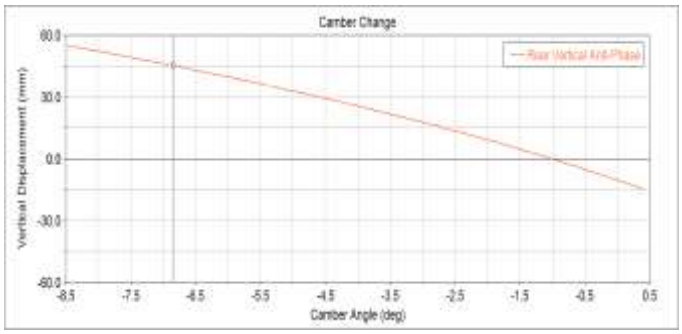

Figure 4.15 Camber Change for Rear suspension during Vertical Anti-Phase.

Above graph shows a non-linear relationship between camber angle and vertical wheel travel when both wheels are displaced anti-phase with the given values of bump and rebound.

- It is seen that the wheels will be in negative camber set up for most of its travel, which is desirable in performance vehicles as they provide great cornering response.
- When the wheel bumps to an extent of 55 mm in vertical direction, the camber angle will decrease to -8.47 degrees.
- When the wheel rebounds to an extent of -15 mm in vertical direction, the camber angle will increase to 0.41 degrees.

Toe Change

Toe can also be described as the difference between the track widths measured at the leading and trailing edges of the tires.

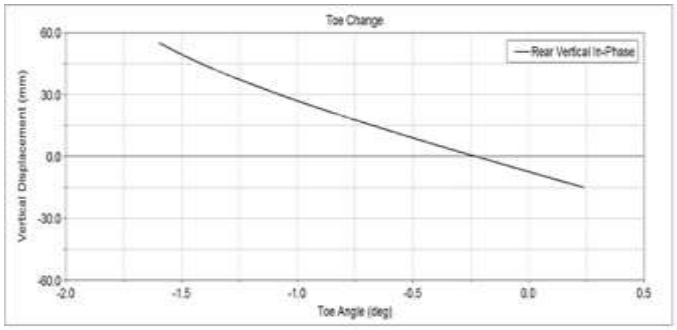

Figure 4.16 Toe Change for Rear suspension during Vertical In-Phase.

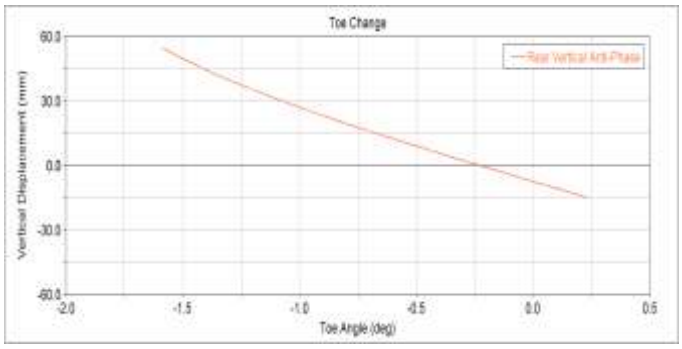

Figure 4.17 Toe Change for Rear suspension during Vertical Anti-Phase.

Above graph shows a non-linear relationship between toe angle and vertical wheel travel during both simulations with the given values of bump and rebound. From the graph, we can observe the following:

- When the wheel bumps to an extent of 55 mm in vertical direction, the toe angle will increase to -1.59 degrees.
- When the wheel rebounds to an extent of -15 mm in vertical direction, the camber angle will decrease non-linearly to 0.2403 degrees.
- Bump results in Toe-out which helps the vehicle to negotiate corners faster and offers less straight line stability.
- Rebound results in Toe-in which is preferred for passenger vehicles as they offer straight line stability. It also helps in achieving under steer characteristics.

V. MAINTAIN ANALYSIS

Maintain analysis or Constant Velocity analysis is a full vehicle analysis performed by automobile engineers to validate the full vehicle built on ADAMS Car.

In Maintain analysis, the full car is made to run along a straight path with a pre-set value of velocity in km/h. A 2D flat road file is used to run the analysis. Here we observe the following,

- Stability of the car and the individual sub systems during the maneuver.
- Behavior of communicators assigned among the different sub systems.
- Weight distribution along the longitudinal axis of the car.
- Forces developed at the tire contact patches.
- Location of CG during maneuver.

By performing maintain analysis, we are able to verify that the location of CG of the virtual prototype conforms closely with the analytical calculations.

The analytical calculations for the physical prototype is shown below.

Analytical Calculation (Physical Prototype)

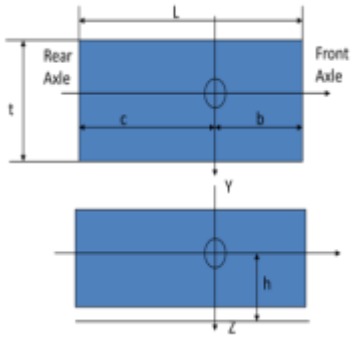

Figure 5.1 Location of C.G in Top and Side views respectively

Sprung Mass = **200 Kg**

Unsprung Mass = **72 Kg**

Total Weight, W = **272 Kg**

Given Weight Distribution = **48:52**

i.e.,

Front Axle Load, Wf = 0.48*272 = **130.5 Kg**

Rear Axle Load, Wr = 0.52*272 = **141.44 Kg**

In static condition,

b= (Wr/W) *L

b= 141.44/272*2100

b= 1092 mm

c= (Wf/W) *L

c=1008 mm

Height of CG, h = 25" = **635mm** (given)

To simulate maintain analysis, the following inputs are taken.

Vehicle	Off-road Rally Vehicle
End Time	10 s
Steps	1000
Road Type	2D flat
Initial Velocity	25 km/hr
Steering Input	Straight Line

Table 5.1 Input data used for Maintain Analysis

After the simulation is complete, we observe the forces developed at each of the four tires in z-direction of the car.

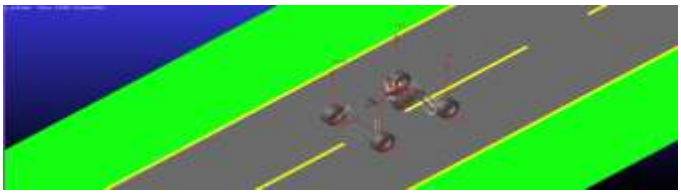

Figure 5.2 Vertical Forces developed at the tire contact patch during maneuver.

Using ADAMS Post Processor, we plot a graph of Normal Force vs Time. Under requests, "wheel tire forces (left and right)" is chosen, and under component, "normal (front and rear) is chosen. This results in the generation of Normal Force vs Time plot as shown.

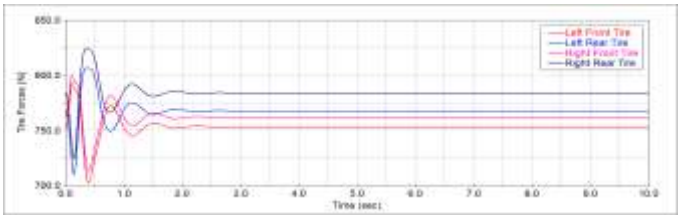

Figure 5.3 Graph of reaction forces developed at tire contact patch w.r.t time

The following forces are obtained at the tire contact patches in z-direction.

Front Left	753 N
Front Right	762 N
Rear Left	767 N
Rear Right	783 N

Table 5.2 Forces at each tire.

To verify the CG location and weight distribution with the analytical results, the following calculations are made.

Total Front Load = 753+762=1515 N

Total Rear Load = 767+783=1550 N

Total Weight = 1515+1550 = 3065 N = 312.4 Kg

Front Load Ratio = 1515/3065 = 0.49 i.e., 49%

Rear Load Ratio = 1550/3065 = 0.51 i.e., 51%

Therefore, Weight Distribution = 49:51

CG location of virtual prototype = (1062.97, 6.92, 436.67)

From the above results, we can observe that the values derived from the MBD model conform closely to the analytically calculated results of the physical prototype.

The table below helps us to get a better idea of this.

Analytical	**MBD**
Sprung Mass = 200 Kg	Sprung Mass = 240 Kg
Unsprung Mass = 72 Kg	Unsprung Mass = 72 Kg
Total Weight = 272 Kg	Total Weight = 312 Kg
Weight distribution = 48:52	Weight distribution = 49:51
Wf = 0.48*272= 130.5 Kg	Wf = 0.49*312= 152.88 Kg
Wr = 0.52*272= 141.44 Kg	Wr = 0.51*312= 159.12 Kg
B = 1092 mm	B = 1062.97 mm
C = 1008 mm	C = 1037.03 mm
H = 635 mm	H = 436.67 mm

Table 5.3 Comparison of Analytical and MBD vehicle specifications

Hence, with the help of maintain analysis, we are able to show close conformity in the weight distribution ratio between virtual and physical prototypes. The location of CG of both versions is also validated. The change in data between the two specimens exists due to limited data available from the actual car.

VI. CONSTANT RADIUS CORNERING

F. Determination of Understeer Gradient Value K:

Constant radius cornering analysis is second of the two full vehicle analysis performed in this project. The virtual prototype is made to maneuver around a circular path with fixed radius. Input vales of initial and final velocities and time are given. This test is conducted to determine the understeer gradient value K.

Understeer gradient is crucial to determine the turning response properties of the car. It shows how the steering angle of the car should be altered with trun radius R, or lateral acceleration (V2/Rg). The equation to determine understeer gradient is given by the expression

$S=57.3*(L/R) + Kay$

$K=(Wf/C\alpha f) - (Wr/C\alpha r)$

Where:

S – Steering angle at front wheel (deg)

L – Wheelbase (mm)

R – Radius of turn (mm)

Wf – Load on front axle (N)

Wr – Load on rear axle (N)

$C\alpha f$ – Cornering stiffness of front tires (N/deg)

$C\alpha r$– Cornering stiffness of rear tires (N/deg)

K – Understeer Gradient (deg/g)

To simulate the constant radius cornering test, the following inputs are given.

Vehicle	Off-road Rally Car
Road	2D flat
Step Size	0.1
Turn Radius	15 m
Turn Direction	Left
Duration of Manoeuvre	17 s
Initial Velocity	10 kmph
Final Velocity	30 kmph

Table 6.1 Input for Constant Radius Cornering analysis.

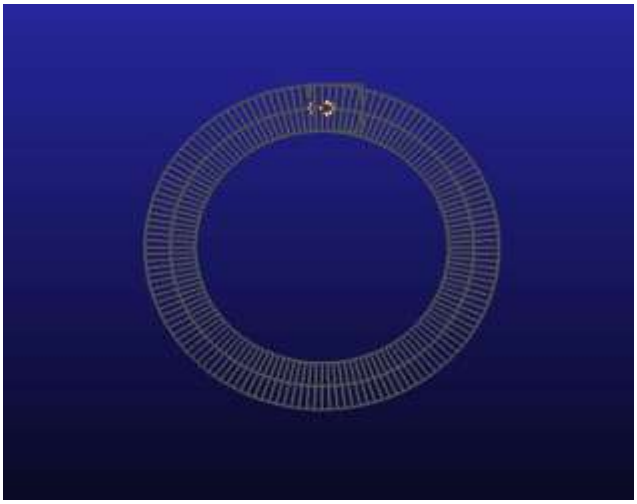

Figure 6.1 Constant Radius Cornering setup

On completion of the simulation, a graph of lateral acceleration vs. steering angle is plotted. The slope of the curve generated gives the value K' i.e., understeer gradient. Depending on the value of K, we can categorize if the vehicle behavior is either of the three,

- Neutral Steer, if K=0
- Understeer, if K>0
- Oversteer, if K<0

In neutral steer condition, no change in steer angle will be required as the speed is varied in a constant radius turn. In understeer condition, the steer angle will have to increase with speed in proportion to K times the lateral acceleration. In over steer condition, the steer angle will have to decrease as the speed is increased.

The following graph shows steer angle vs lateral acceleration plotted for the virtual prototype of the rally car in Constant Radius Cornering test.

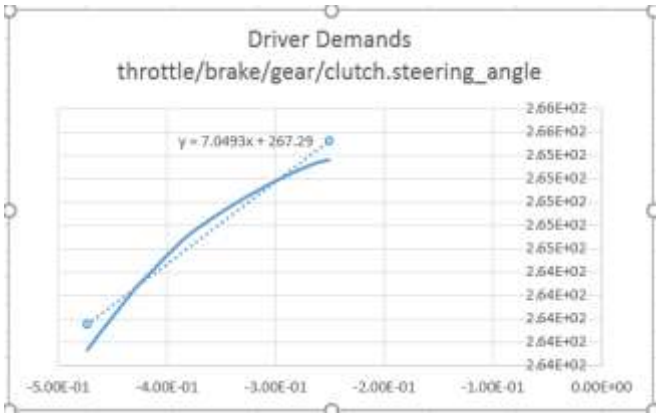

Figure 6.2 Understeer Gradient Characteristic Curve

From the behavior of the graph we can see the slope value K is positive as the curve resembles the straight line of equation y = mx + c, where m is K.

Since K is positive, we can conclude that the vehicle behavior is understeer for constant radius of turn with varying speeds. The value of K is approximately = 7.04 deg/g

G. Forces developed in Lower Control Arm (LCA):

The forces generated in the control arms are usually the highest during cornering. Hence, to understand the magnitude and range forces developed, we observe the axial forces acting on the lower control arm pivots, where the control arms connect to the chassis. The two locations where we observe the axial forces in x, y and z directions are:

- LCA front
- LCA rear

Both the LCAs, i.e., on the left and right, are considered.

The following inputs are given to simulate Constant Radius Cornering Analysis.

Vehicle	Off-road Rally Car
Road	2D flat
Step Size	0.1
Turn Radius	15 m
Turn Direction	Left
Duration of Manoeuvre	17 s
Initial Velocity	10 kmph
Final Velocity	30 kmph

Table 6.2 Input for CRC analysis to optimize forces developed in the control arm links.

A graph of LCA front and LCA rear forces vs time is plotted. In order to reduce these forces acting in the control arms, by trial and error, an observation was recorded to show that the forces actually decreased in the control arms when the distance between the LCA front and LCA rear links were further increased in x direction. The two pivots were parted further away from each other by 40mm in x direction.

Entity	Original Location	Modified Location
LCA Front(Left)	-120,-320,170	-140,-320,170
LCA Rear (Left)	75,-345,180	95,-345,180
LCA Front(Right)	-120,320,170	-140,320,170
LCA Rear (Right)	75,345,180	95,345,180

Table 6.3 Modified Hard Point locations of Lower Control Arm.

Figure 6.2 Top View of Original and Modified suspension arm location.

This adjustment in design is done so that the forces are reduced in the control arms. Since in the physical prototype, the front link of the LCA on right side has failed, we observe the forces Fx, Fy, and Fz developed in that link. The forces Fx, Fy and Fz are observed vs time.

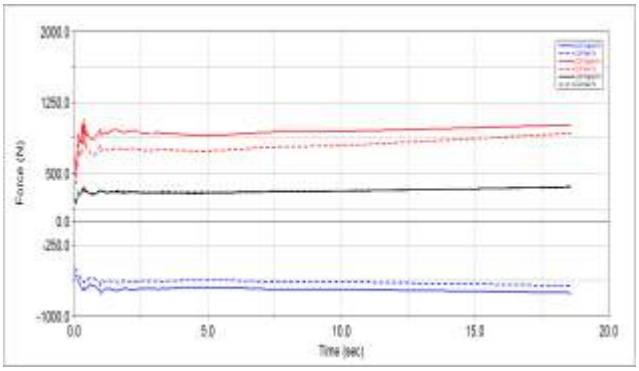

Figure 6.3 Graph of forces developed in the front link of right arm during cornering w.r.t time.

From the above graph it can be observed that the forces in LCA right front link have reduced in the updated design compared to the original design.

We know that,

Torque(T)= Force(F) * Perpendicular Distance(d)

Since the distance between the two links pivots have been increased, the distance between the point of action of force and the center have also increased. As a result, the effort or force, required to generate the same torque now decreases. This explains the reduction of forces in the link pivots.

The following data shows the values of forces acting in the front link of Right sided LCA.

Fx Original	-700 N
Fx Modified	-620 N
Fy Original	910 N
Fy Modified	748 N
Fz Original	300 N
Fz Modified	307 N

Figure 6.4 Forces developed in the front link of right arm during cornering.

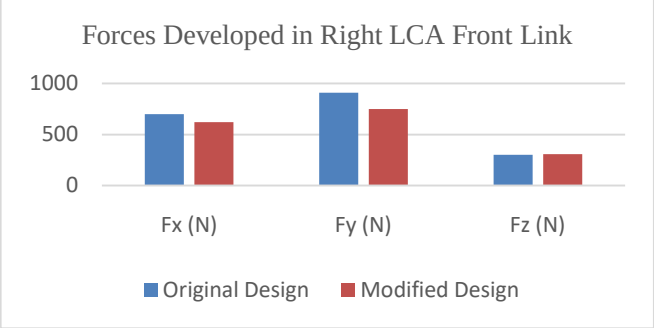

Figure 6.5 Bar Graph depicting the decrease in forces developed in the modified design

Percentage reduction in Fx	11.43 %
Percentage reduction in Fy	17.81 %
Percentage increase in Fz	2.29 %

Table 6.5 Percentage change in forces developed in the front link of right arm.

These improvements shown by altering the design of the LCA are found to be considerable in forces acting in longitudinal and lateral directions at the pivots. However, the forces acting in the vertical direction remain the same. With this modification, we can show that the chance of failure of the lower control arm solely due to dynamic forces produced during maneuver has been decreased.

VII. Flex Body Analysis

All the analyses carried out till this stage have been run by using rigid bodies. The flexibility of these bodies are not showing their influence on the MBD results as every part is assumed to behave rigidly upon application or development of forces.

To understand the reason for failure in the lower control arm in the actual model, we need to understand the stress levels acting in the LCA during any maneuver. This can be done by incorporating a flexible body, in this case, a flexible LCA on both sides of the car. The rigid body is replaced with the flexible body to run the simulation.

H. Generation of Flexible Lower Control Arm:

To replace the rigid body with a flexible component, software tools such as MSC Apex, MSC Patran and MSC Nastran have been used.

The following steps were taken to create flexible LCA on both sides.

- The rigid LCA is exported as an iges file.
- This file is imported into MSC Apex, which is a CAD tool used for modelling and simple meshing.
- The different links in the LCA are merged together to form one geometry. This is done using the Boolean feature.
- A tetrahedral mesh with the following mesh attributes is used.

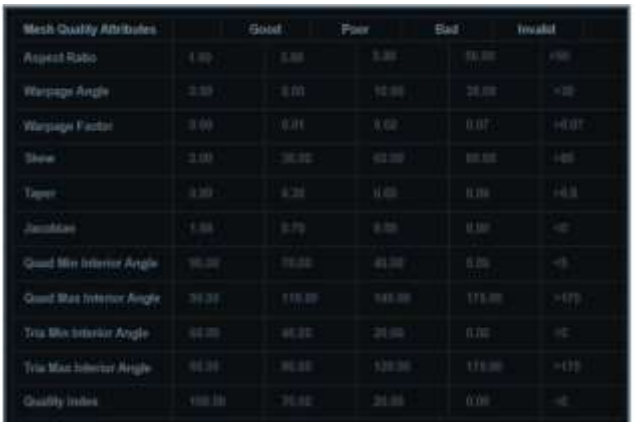

Figure 7.1 Mesh Attributes used while preparing a flexible arm

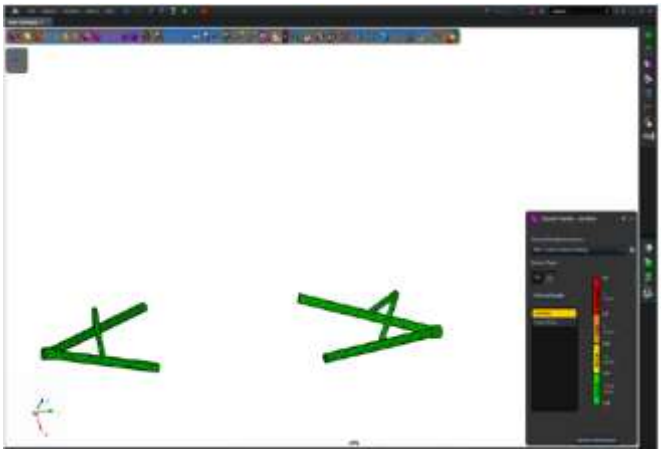

Figure 7.2 Geometry of arm after Boolean and meshing process.

- Once meshing is done, the file is exported as a parasolid and taken into MSC Patran.
- MSC Patran is a pre-processing FEA software tool used to generate mesh, assign properties etc.,
- The model is given three multipoint constraints at the locations where the LCA is pivoted to the knuckle and frame. This is done so that relative motion between the flexible part and the connecting rigid part exists after meshing.
- This file is then taken into MSC Nastran, which is a post-processing FEA tool, to generate the Modal Neutral File or MNF file.
- We can now easily replace the rigid body with the MNF file of the flexible part on ADAMS Car.

I. Constant Radius Cornering using Flexible Lower Control Arm:

Upon generation of the MNF file of the lower control arms, the rigid arms are swapped with the flexible ones on Adams Car. From now on, the stresses and deformation experienced by the LCA will play a role in any simulation the car is made to operate in.

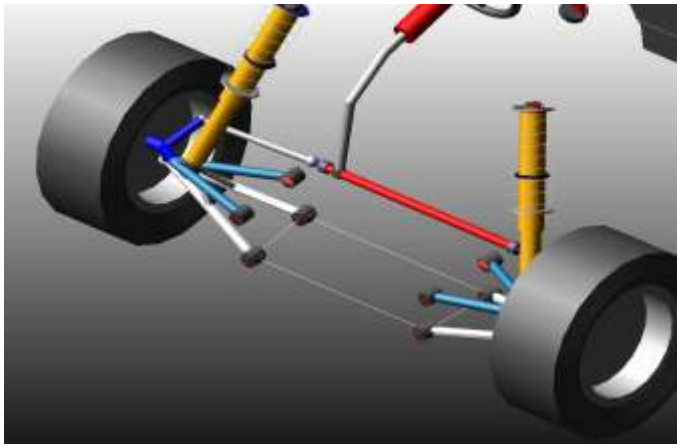

Figure 7.3 Flexible Arms imported into the original assembly.

During maneuvering of the car, the control arms experience the greatest forces when the vehicle is experiencing a cornering event. Hence, to see if the arm has failed due to the dynamic forces generated during cornering, a CRC test is simulated with the flexible arms as part of the assembly.

To simulate the constant radius cornering test, the following inputs are given.

Vehicle	Off-road Rally Car
Road	2D flat
Step Size	0.1
Turn Radius	15 m
Turn Direction	Left
Duration of Manoeuvre	14 s
Initial Velocity	10 kmph
Final Velocity	30 kmph

Table 7.1 Input for CRC analysis using flexible body.

After simulation, using Adams Durability plugin, the hotspots in the control arm on the right side can be observed. Hotspots are the nodes at which there are highest stresses are acting. Von Mises stresses in the arm are observed during CRC test. The hotspots table for right sided LCA are given as follows.

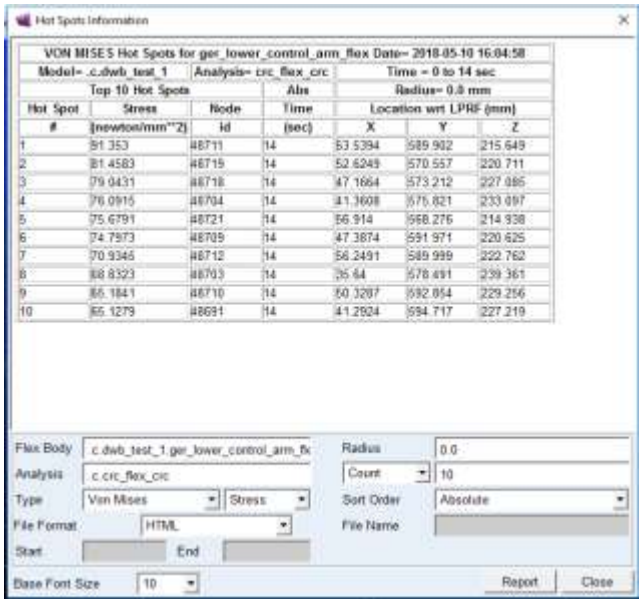

Figure 7.4 Hotspots of Von Mises stresses on the right LCA.

It is seen that the maximum Von Mises stress acting on the arm is around 91.3 MPa. This region which is experiencing the highest stress value is shown in the figure below.

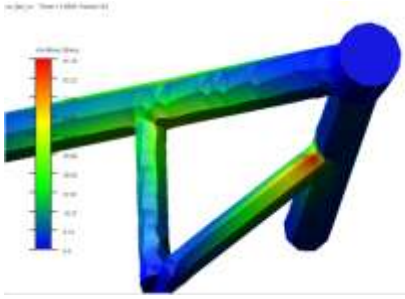

Figure 7.5 High stress region in the lower control arm.

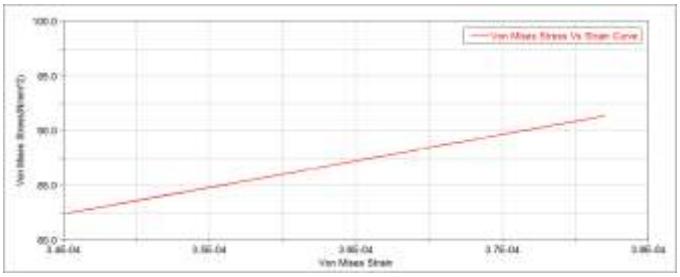

Figure 7.6 Stress Strain curve to observe Von Mises stresses in the right LCA.

The graph shows Von Mises stress strain curve of the LCA on the right side during CRC test. It is seen that the maximum stress developed in the arm is around 91.3 MPa. It is clear from the plot that stress is directly proportional to strain and the material is still behaving elastically. The yielding will only start to take place at 250 MPa for steel.

Hence, it is proved that the control arm failure is not related to any dynamic loading during the maneuver. There are other reasons that could have caused failure in the arm.

On observing the failure area in the real car, it is seen that the arm has failed at the place of weld used to connect two bodies of the link.

The welding region clearly looks like it has been welded with bad welding techniques.

Bad welds lead to voids and sharp corners in the material. These act as high stress concentration regions which are prone to act as sources of macroscopic crack sites. The cracks have propagated through the weld seam upon vehicle dynamic loading and have ultimately given in structurally.

VIII. Conclusion and Future Scope

J. Conclusion

Modelling of the vehicle has been carried out by referring the hardpoints. The hard points are extracted from the physical prototype using a measure tape accurately. Using these data, the template for front, rear suspensions and steering are created. The subsystems are developed from this and the full car assembly is created using Adams Car.

Validation of the individual suspension systems have been carried out. The front and rear suspension subsystems have been validated using Kinematics analysis. The MBD model conforms closely with the physical prototype. Along with this, full vehicle analyses are conducted following the validation of individual suspension subsystems.

In Full Vehicle analyses, Maintain Analysis is conducted to observe the reaction forces produced at the tire contact patch when the vehicle is travelling at constant velocity along a straight path. Using this analysis, a close conformity in the results is observed between the MBD model and Physical car when the location of CG was closely observed.

Constant Radius Cornering analysis is conducted to determine the understeer gradient. It is observed that the car behaves with understeer conditions. The forces generated in the front LCA right arm front link are observed during cornering. The design of the Lower Control Arm is slightly modified and CRC test is conducted. The forces developed in the right LCA front link is observed to be lesser in the modified design compared to the original design.

To analyze the failure in right LCA front link, flexible body analysis is carried out using MSC Apex, MSC Nastran and MSC Patran. The resulting Modal Neutral File is switched for the rigid LCA on right and left side. Using Adams Durability, the Hot Spots table is generated to see the highest stress developed at the corresponding node and the von mises stress vs strain graph is plotted. It is clearly observed that the arm experiences only a max of 91 MPa stress and still behaves elastically, i.e., yielding has not started. With this it is concluded that the LCA in the rally car has not failed due to any dynamic loads duringmaneuver. Reason for failure can be due to poor welding techniques and manufacturing processes employed.

K. Scope for Future Work.

- Hook Joints can be used to mount the struts instead of welding them to the chassis thus providing the suspension with extra degrees of freedom to actuate.
- Bushes with known optimum values can be used in places necessary to conduct Compliance part of K and C analysis.
- The K and C analysis can be conducted physically using SPMM (Suspension Parameter Measuring Machine) test rig. The results obtained can be plotted over the MBD results to see the close conformity more clearly.
- The suggested improvement in design of the LCA can be fabricated and employed into the physical car to see improvement in results.
- Control arms can be employed into the rear suspension of the physical car to see improvement in the handling characteristics.

References

[1] Samuel Joseph (2013), Design and Development of Steering and Suspension System of a Concept Car.
[2] Thomas D. Gillespie (1992), Fundamentals of Vehicle Dynamics, Society of Automotive Engineers Inc.
[3] Richard Stone and Geoffrey K. Ball (2004), Automotive Engineering Fundamentals, SAE International.
[4] Shaopu Yang, Yongjie Lu and Shaohua Li (2013), An overview on vehicle dynamics, Springer-Verlag Berlin Heidelberg.
[5] Emre Sert and Pınar Boyraz (2017), Optimization of Suspension System and Sensitivity Analysis forImprovement of Stability in a Midsize Heavy Vehicle, Engineering Science and Technology, an International Journal.
[6] Anoop M. Vasudevan and Jithin Bhaskar, A study on the Handling Characteristics of a Car during Cornering with Variation in Wheel Geometry Parameters, VIT University, Vellore.
[7] Sarel F. van der Westhuizen, Pieter S. Els (2012), Slow active suspension control for rollover prevention, Journal of Terramechanics.
[8] N. Ikhsan, R.Ramli and A. Alias (2015), Analysis of the kinematics and compliance of a passive suspension system using Adams Car, Journal of Mechanical Engineering and Sciences